Enhanced Radio Frequency Carrier Margin Improvement for an Array of Receiving Systems with Unequal Predetection Signal-to-Noise Ratios

M. H. Brockman
Telecommunications Science and Engineering Division

Enhanced radio frequency carrier margin improvement for arrayed receiving systems for coherent reception provides a significant carrier sensitivity improvement with a resultant decrease in telemetry radio loss due to reduction in rms phase noise at low carrier margins. In addition, a significant increase in doppler rate capability is realized relative to that obtained by switching to a narrower tracking loop bandwidth to obtain the same carrier sensitivity improvement. This report examines this situation for arrayed receiving systems with unequal apertures and statistically independent predetection noise.

I. Introduction

This report presents a technique for providing enhanced radio frequency carrier margin improvement for coherent carrier reception and demodulation for an array of receiving systems with unequal antenna apertures. A later report will present enhanced RF carrier margin improvement for an array with equal antenna apertures. In this initial report, the various components of operating system noise temperature are treated as statistically independent among the receiving systems of the array. Later reports will examine the effect of partial coherence in system noise temperature on enhanced carrier margin improvement for an array of receiving systems with unequal antenna apertures and for an array with equal antenna apertures. Performance presented herein for enhanced RF carrier margin improvement is representative of 34-m diameter antenna receiving systems arrayed with a 64-m diameter antenna receiving system which also has transmit capability.

II. Receiver Configuration

Figure 1 illustrates a configuration considered herein which is the same as that shown in Fig. 1 (Ref. 1) except that the noise bandwidth of predetection IF filters F_{A_2} through F_{A_N} in receiving systems 2 through N are k times the noise bandwidth of predetection IF filter F_{A_1} in receiving system 1 where k is larger than 1. Figure 1 and a modification of Fig. 1 (so that much larger antenna separations for the array can be handled conveniently) were presented in Ref. 2 with a discussion of predetection noise resulting from operating equivalent system noise temperature (T_{o_p}). Figure 2 illustrates a second configuration that provides additional filtering of receiving system 2 (through N) local oscillator phase noise which couples into receiving system 1 via the RF carrier summing junction shown. As a consequence, Fig. 2 generally provides an increase in enhanced carrier margin improvement relative to that obtained utilizing Fig. 1.

III. Predetection Signal-to-Noise Ratio and RF Carrier Tracking Loop Phase Noise

For the situation considered herein, the improvement in predetection signal-to-noise ratio that was developed in Ref. 1, (Eq. 3) for an array of two receiving systems and (Eq. 5) for an array of N receiving systems, represents the improvement in predection carrier power to noise spectral density ratio for the RF carrier phase tracking loop in receiving system 1. These expressions in Ref. 1 apply for the case where a portion of the predetection noise is coherent (ϵ_1 and ϵ_2 in receiving systems 1 and 2, respectively). In this initial report, however, the various components of system noise are treated as statistically independent so that ϵ_1 and ϵ_2 are zero and $1 - \epsilon_1 = 1 - \epsilon_2 = 1$. The improvement in predetection carrier power to noise spectral density ratio in receiving system 1 for two receiving systems arrayed (n_2) then becomes

$$n_2 = \frac{(1 + \beta_2 \gamma_2)^2}{\left[1 + \frac{N_{o2}}{N_{o1}} \beta_2^2\right]} \tag{1}$$

where β_2 is the voltage coupling of receiving system 2 relative to receiving system 1 at the summing junction and γ_2^2 is the carrier power-to-noise spectral density ratio of receiving system 2 relative to receiving system 1. The term N_{o1} is the one-sided noise spectral density of receiving system 1 related to T_{op_1} and N_{o2} is the noise spectral density of receiving system 2 related to T_{op_2}. For N receiving systems arrayed, the improvement in predetection carrier power to noise spectral density ratio (n_N) in receiving system 1 then becomes

$$n_N = \frac{(1 + \beta_2 \gamma_2 + \cdots \beta_N \gamma_N)^2}{\left[1 + \frac{N_{o2}}{N_{o1}} \beta_2^2 + \cdots + \frac{N_{oN}}{N_{o1}} \beta_N^2\right]} \tag{2}$$

Reference 1 provides detailed performance information on improvement in predetection signal-to-noise ratio.

Consider the RF carrier phase tracking loop in receiving system 1 for the situation where the predetection IF filters F_{A_2} through F_{A_N} in receiving systems 2 through N have k times the noise bandwidth of predetection IF filter F_{A_1} (Fig. 1). The carrier tracking loop is a second-order phase tracking loop which includes a bandpass limiter and a sinusoidal phase detector. With receiving system 1 only connected to the summing junction, the RF carrier signal-to-noise power ratio at the input to the bandpass limiter is (Ref. 2, Eq. 1)

$$\frac{P_{c1}}{P_{n1}} = \frac{(A_1 \cos m_{pD})^2}{NBW_{F_{A1}} \cdot N_{o1}} \text{ or } \frac{P_{c1}}{NBW_{F_{A1}} \cdot N_{o1}} \tag{3}$$

where m_{pD} is the peak phase modulation index and $NBW_{F_{A1}}$ represents the noise bandwidth of predetection IF filter F_{A1}. The resultant rms phase noise (σ_{ϕ_n}) at the output of the RF carrier tracking loop (i.e., on the first local oscillator) can be expressed as

$$\sigma_{\phi_{n1}} = \underbrace{\left(\frac{\frac{N_{o1}}{2} \cdot 2B_{L1}}{P_{c1}}\right)^{1/2}}_{\text{(a)}} \cdot \underbrace{\left[\frac{1 + \frac{P_{c1}}{NBW_{F_{A1}} N_{o1}}}{0.862 + \frac{P_{c1}}{NBW_{F_{A1}} N_{o1}}}\right]^{1/2}}_{\text{(b)}}$$

$$\cdot \underbrace{\left[\frac{N_{o1} B_{L1}}{P_{c1}} \cdot \frac{\exp\left(\frac{N_{o1} B_{L1}}{P_{c1}}\right)}{\sinh\left(\frac{N_{o1} B_{L1}}{P_{c1}}\right)}\right]^{1/2}}_{\text{(c)}} \text{ rad, rms} \tag{4a}$$

for $\sigma_{\phi_n} \leqslant 1$ rad rms. Collecting terms, Eq. (4a) becomes (Ref. 2, Eq. 2)

$$\sigma_{\phi_{n1}} = \frac{\frac{N_{o1}}{2} \cdot 2B_{L1}}{P_{c1}} \cdot \left[\frac{1 + \frac{P_{c1}}{NBW_{F_{A1}} \cdot N_{o1}}}{0.862 + \frac{P_{c1}}{NBW_{F_{A1}} \cdot N_{o1}}} \cdot \frac{\exp\left(\frac{N_{o1} B_{L1}}{P_{c1}}\right)}{\sinh\left(\frac{N_{o1} B_{L1}}{P_{c1}}\right)}\right]^{1/2} \text{ rad, rms} \tag{4b}$$

The two-sided closed-loop noise bandwidth can be expressed as

$$2B_{L1} = \frac{2B_{Lo1}}{r_o + 1}\left(1 + r_o \frac{\alpha_1}{\alpha_{o1}}\right) \tag{5}$$

where $r_o = 2$ by design at design point (0.707 damping) and $2B_{Lo1}$ is the design point (threshold) two-sided closed-loop

noise bandwidth in receiving system 1. The term α_1 is the limiter suppression factor resulting from the noise-to-carrier power ratio due to $NBW_{F_{A1}}$ at the input to the bandpass limiter. The suppression factor α_1 has a value of α_{o1} at design point (threshold). At threshold, the predetection carrier-to-noise power ratio in a noise bandwidth equal to $2B_{L_{o1}}$ is unity (i.e., $P_c/(2B_{Lo} \cdot N_o) = 1$). Note that the term designated (b) in Eq. (4a) is determined by the carrier-to-noise power ratio at the input to the bandpass limiter.

With receiving systems 1 and 2 connected to the summing junction, the RF carrier signal-to-noise power ratio at the input to the bandpass limiter is (Ref. 1, Eq. 1 with ϵ_1 and $\epsilon_2 = 0$)

$$\frac{P_{c1_{\Sigma 1,2}}}{P_{n1_{\Sigma 1,2}}} = \frac{(A_1 \cos m_{pd} + \beta_2 A_2 \cos m_{pd})^2}{\left[NBW_{F_{A1}} \cdot N_{o1} + \beta_2^2 MBW_{F_{A2}} \cdot N_{o2}\right]} \tag{6}$$

where $NBW_{F_{A2}} = k_2 \cdot NBW_{F_{A1}}$. Equation (6) can be rewritten as

$$\frac{P_{c1_{\Sigma 1,2}}}{P_{n1_{\Sigma 1,2}}} = \frac{P_{c1}}{NBW_{F_{A1}} \cdot N_{o1}} \cdot \frac{(1 + \beta_2\gamma_2)^2}{\left[1 + \frac{N_{o2}}{N_{o1}} \beta_2^2 k_2\right]} \tag{7}$$

The change in RF carrier signal-to-noise power ratio at the input to the bandpass limiter in receiving system 1 is then (comparison of Eqs. [7] and [3]):

$$\Delta_2 = \frac{(1 + \beta_2\gamma_2)^2}{\left[1 + \frac{N_{o2}}{N_{o1}} \beta_2^2 k_2\right]} \tag{8}$$

The limiter suppression factor due to the change in noise-to-carrier power ratio becomes $\alpha_{1_{\Delta 2}}$ which provides a two-sided closed-loop noise bandwidth:

$$2B_{L1_{\Delta 2}} = \frac{2B_{L_{o1}}}{r_o + 1}\left(1 + r_o \frac{\alpha_{1_{\Delta 2}}}{\alpha_{o1}}\right) \tag{9}$$

The resultant rms phase noise at the output of the RF carrier tracking loop (i.e., on the first local oscillator) in receiving system 1 becomes:

$$\sigma_{\phi_{n1\Sigma 1,2}} = \frac{\frac{N_{o1}}{2} \cdot 2B_{L1_{\Delta 2}}}{P_{c1}} \cdot \frac{1}{n_2} \cdot \left[\frac{1 + \frac{P_{c1} \cdot \Delta_2}{NBW_{F_{A1}} \cdot N_{o1}}}{0.862 + \frac{P_{c1} \cdot \Delta_2}{NBW_{F_{A1}} \cdot N_{o1}}} \cdot \frac{\exp\left(\frac{N_{o1} \cdot B_{L1_{\Delta 2}}}{P_{c1} \cdot n_2}\right)}{\sinh\left(\frac{N_{o1} \cdot B_{L1_{\Delta 2}}}{P_{c1} \cdot n_2}\right)}\right]^{1/2} \tag{10}$$

For N receiving systems connected to the summing junction, the RF carrier signal-to-noise power ratio at the input to the bandpass limiter becomes

$$\frac{P_{c1\Sigma 1,\ldots,N}}{P_{n1\Sigma 1,\ldots,N}} = \frac{P_{c1}}{NBW_{F_{A1}} \cdot N_{o1}} \cdot \frac{(1 + \beta_2\gamma_2 + \cdots + \beta_N\gamma_N)^2}{\left[1 + \frac{N_{o2}}{N_{o1}} \beta_2^2 k_2 + \cdots + \frac{N_{oN}}{N_{o1}} \beta_N^2 k_N\right]} \tag{11}$$

The change in RF carrier signal-to-noise power ratio at the input to the bandpass limiter in receiving system 1 is (comparison of Eqs. [11] and [3]):

$$\Delta_N = \frac{(1 + \beta_2\gamma_2 + \cdots + \beta_N\gamma_N)^2}{\left[1 + \frac{N_{o2}}{N_{o1}} \beta_2^2 k_2 + \cdots + \frac{N_{oN}}{N_{o1}} \beta_N^2 k_N\right]} \tag{12}$$

The limiter suppression factor becomes $\alpha_{1_{\Delta N}}$ which provides a two-sided closed-loop noise bandwidth

$$2B_{L1_{\Delta N}} = \frac{2B_{L_{o1}}}{r_o + 1}\left(1 + r_o \frac{\alpha_{1_{\Delta N}}}{\alpha_{o1}}\right) \tag{13}$$

For N receiving systems arrayed, the resultant rms phase noise becomes:

$$\sigma_{\phi_{n1\Sigma\,1,\ldots,N}} = \frac{\frac{N_{o_N}}{2} \cdot 2B_{L1_{\Delta N}}}{P_{c1}} \cdot \frac{1}{n_N}$$

$$\cdot \left[\frac{1 + \frac{P_{c1} \cdot \Delta_N}{NBW_{F_{A1}} \cdot N_{o1}}}{0.862 + \frac{P_{c1} \cdot \Delta_N}{NBW_{F_{A1}} \cdot N_{o1}}} \cdot \frac{\exp\left(\frac{N_{o1} \cdot B_{L1_{\Delta N}}}{P_{c1} \cdot n_N}\right)}{\sinh\left(\frac{N_{o1} \cdot B_{L1_{\Delta N}}}{P_{c1} \cdot n_N}\right)} \right]^{1/2} \text{rad, rms} \tag{14}$$

Note that the total rms phase noise at the output of the RF carrier tracking loop (i.e., on the first local oscillator) in receiving system 1 for Fig. 1 is

$$\left[\sigma^2_{\phi_{n1\Sigma\,1,2}} + \left(\frac{\beta_2 \sigma_{\phi_{n2}}}{1 + \beta_2} \right)^2 \right]^{1/2} \tag{15}$$

for two receiving systems arrayed (Ref. 2). For N receiving systems arrayed, the total rms phase noise for Fig. 1 is

$$\left[\sigma^2_{\phi_{n1\Sigma\,1,\ldots,N}} + \left(\frac{\beta_2 \sigma_{\phi_{n2}}}{1 + \beta_2} \right)^2 + \cdots + \left(\frac{\beta_N \sigma_{\phi_{nN}}}{1 + \beta_N} \right)^2 \right]^{1/2} \tag{16}$$

Expressions for rms phase noise in the carrier phase tracking in receiving systems 2 through N were developed in Ref. 2.

In Fig. 2, additional filtering of the output rms phase noise $\sigma_{\phi_{n2}}$ is provided by the local oscillator tracking loop in receiving system 2. Designate the additionally filtered rms phase noise as $\sigma'_{\phi_{n2}}$ which is less than $\sigma_{\phi_{n2}}$ by the square root of the ratio of local oscillator tracking loop noise bandwidth to $2B_{L2}$. Consequently for Fig. 2, $\sigma'_{\phi_{n2}}$ and $\sigma'_{\phi_{nN}}$ are substituted into Eqs. (15) and (16) in place of $\sigma_{\phi_{n2}}$ and $\sigma_{\phi_{nN}}$.

The rms phase noise ($\sigma_{\phi n1}$) for receiving system 1 by itself is determined, using Eq. (4), from threshold to stronger RF carrier levels for a given set of parameters. A given RF carrier level above threshold (carrier margin) results in a specific $\sigma_{\phi_{n1}}$ at the output of RF carrier phase tracking loop in receiving system 1. With receiving system 1 and 2 connected to the summing junction, total rms phase noise at the output of the RF carrier tracking loop in receiving system 1 is determined from Eqs. (10) and (15). The rms phase noise, Eqs. (15) and (10), represents a different RF carrier margin when compared to $\sigma_{\phi_{n1}}$ for receiving system 1 alone. The change in carrier margin represents the enhanced carrier margin improvement in receiving system 1 for two receiving systems arrayed. With N receiving systems arrayed, Eqs. (16) and (14) represent the change in RF carrier margin relative to receiving system 1 alone to provide the enhanced carrier margin improvement in receiving system 1 for N receiving systems arrayed. Note that receiving systems 2 through N have essentially the same RF carrier characteristics and sensitivity as receiving system 1.

IV. Performance

The enhanced RF carrier margin improvement that can be obtained by arraying receiving systems can now be determined for representative sets of design parameters using the preceding development. The following sets of design parameters apply for the performance presented in this report. The sets of design parameters for receiving system 1 are:

Threshold Two-Sided Noise Bandwidth				
$2B_{L_{o1}}$	10.0	30.0	100.0	300.0 Hz
Predetection IF Filter Noise Bandwidth				
$NBW_{F_{A1}}$	2000.0	2000.0	20000.0	20000.0 Hz

while the corresponding sets of parameters for receiving system 2 through N are:

Threshold Two-Sided Noise Bandwidth				
$2B_{L_{o2,\ldots,N}}$	0.3	1.0	3.0	10.0 Hz
Predetection IF Filter Noise Bandwidth				
$NBW_{FA2,\ldots,N}$	$k \cdot NBW_{F_{A1}}$	$k \cdot NBW_{F_{A1}}$	$k \cdot NBW_{F_{A1}}$	$k \cdot NBW_{F_{A1}}$
Local Oscillator Tracking Loop Two-Sided Noise Bandwidth (Fig. 2)				
	1.0	1.0	1.0	1.0 Hz

Using the bandwidth parameters above and the array parameters described below, the enhanced RF carrier margin improvement for receiving system 1 is presented in the following material which is representative of 34-m diameter antenna receiving system(s) arrayed with a 64-m diameter antenna receiving system (system 1).

Figure 3 shows enhanced RF carrier margin improvement for receiving system 1 for array configurations representative

of Figs. 1 and 2 as a function of k (where k is the ratio NBW_{FA2}/NBW_{FA1}) with the summing junction voltage coupling β_2 equal to one and $2B_{L_{o1}}$ = 10.0 Hz. Figure 3 represents an array of two receiving systems with a 64-m diameter antenna (system 1) and a 34-m diameter antenna-listen only (system 2) with γ_2 = 0.61 (-4.3 dB). As described earlier in this report, γ_2^2 is the carrier power-to-noise spectral density ratio of receiving system 2 relative to receiving system 1. For Fig. 3, receiving system 1 by itself prior to arraying has an RF carrier level 10 dB above design point threshold (10 dB RF carrier margin), and a two-sided closed loop noise bandwidth of 24.5 Hz for the RF carrier phase tracking loop at this carrier level. The ratio of noise spectral densities (N_{o2}/N_{o1}) (of receiving system 2 relative to receiving system 1) is 0.925 (18.5 K/20.0 K) for noncoherent predetection noise ($(1 - \epsilon_1) = 1$).

Note that in Fig. 3, the enhanced RF carrier margin improvement for receiving system 1 increases to 7.8 dB (when k becomes 27) for array configurations representative of Figs. 1 or 2. Since γ_2 = 0.61 for system 2, the corresponding enhanced RF carrier margin improvement for receiving system 2 is 12.1 dB (for k = 27) relative to receiving system 2 by itself operating with a $2B_{L_o}$ of 10 Hz. At k = 27 (Fig. 3), the two-sided closed-loop noise bandwidth of the RF carrier tracking loop in receiving system 1 is 10 Hz (design point noise bandwidth).

The information shown in Fig. 3 is rearranged and expanded in Fig. 4 to show enhanced RF carrier margin improvement for receiving system 1 as a function of the RF carrier level in dB above threshold (carrier margin) of receiving system 1 by itself prior to arraying for selected values of k. Enhanced RF carrier margin improvement is shown for values of k equal to 3.5, 9, 16, 27, and 70 for the two receiving systems arrayed. For k = 9 (Fig. 4), the initial RF carrier level for receiving system 1 by itself prior to arraying must be at least 5.5 dB above threshold. At this 5.5 dB level and with the two receiving systems arrayed, the two-sided closed loop noise bandwidth of the RF carrier tracking loop in receiving system 1 is 10 Hz (design point noise bandwidth). Consequently, the doppler and doppler rate characteristics vs. received carrier level of the RF carrier tracking loop for the array (k = 9) are transferred (moved) 5.5 dB to the right relative to receiving system 1 operation by itself. At this 5.5 dB carrier level, the enhanced RF carrier margin improvement (for k = 9) is 5.3 dB for array configurations representative of Figs. 1 and 2. For k = 16, 27, and 70, the initial RF carrier level of receiving system 1 by itself prior to arraying must be at least 8 dB, 10 dB, and 14 dB above threshold respectively. The doppler and doppler rate characteristics vs. received carrier level of the RF carrier tracking loop for the array are transferred (moved) 8 dB, 10 dB and 14 dB respectively to the right for k = 16, 27, and 70 as described above.

Figures 5 and 7 show performance characteristics (which are similar to those in Figs. 3 and 4) for an array of two receiving systems utilizing a 64-m diameter antenna and a 34-m diameter antenna-listen only. For this array, receiving system 1 has a $2B_{L_{o1}}$ of 30 Hz for the RF carrier phase tracking loop. For Fig. 5, receiving system 1 by itself prior to arraying has a 10 dB RF carrier margin and a two-sided closed loop noise bandwidth of 70.2 Hz for the RF carrier phase tracking loop at this carrier level. At k = 36 (Fig. 5), the two-sided closed loop noise bandwidth of the RF carrier tracking loop in receiving system 1 is 30 Hz (design point noise bandwidth) and the enhanced RF carrier margin improvement is 7.1 and 7.2 dB for array configurations representative of Figs. 1 and 2, respectively. Figure 6 shows the effect of varying the voltage coupling β_2 of receiving system 2 relative to receving system 1 at the summing junction on enhanced RF carrier margin improvement for k = 18.

In Fig. 7 ($2B_{L_{o1}}$ = 30 Hz), enhanced RF carrier margin improvement for receiving system 1 is shown for values of k equal to 3.5, 9, 18, 36, and 70. In this case, the initial RF carrier level for receiving system 1 prior to arraying must be at least 5.5, 8, 10, and 14 dB above threshold for k equal to 9, 18, 36, and 70, respectively. As before, the doppler and doppler rate characteristics vs. received carrier level for the array are transferred (moved) a corresponding amount to the right in RF carrier level relative to receiving system 1 by itself prior to arraying.

Figures 8 and 9 show enhanced RF carrier margin improvement characteristics (similar to Figs. 3 and 4) for two receiving systems arrayed (64-m diameter antenna and 34-m diameter-listen only antenna) with receiving system 1 operating with a $2B_{L_{o1}}$ of 100 Hz. Figures 10 and 11 show performance characteristics (similar to Figs. 5 and 7) for the case where $2B_{L_{o1}}$ = 300 Hz. It should be noted that for the sets of design parameters considered in this report, enhanced RF carrier margin improvement for a $2B_{L_{o1}}$ for 100 Hz and 300 Hz are the same as for a $2B_{L_{o1}}$ of 10 Hz and 30 Hz respectively for a configuration representative of Fig. 1.

Consider the case for an array of three receiving systems consisting of a 64-m diameter antenna (system 1), a 34-m diameter antenna-listen only (system 2) and a 34-m diameter antenna with transmit/receive capability (system 3). As described above, γ_2 is 0.61 (-4.3 dB) and N_{o2}/N_{o1} is 0.925 for receiving system 2 relative to receiving system 1. For receiving system 3, γ_3 is 0.53 (-5.5 dB) and N_{o3}/N_{o1} is 1.075 (21.5 K/20.0 K) relative to receiving system 1 for noncoherent predetection noise ($(1 - \epsilon_1) = 1$). Enhanced RF carrier margin

improvement is presented in Figs. 12 and 13 for a $2B_{L_{o1}}$ = 10 Hz; Figs. 14 and 15 for a $2B_{L_{o1}}$ = 30 Hz; Figs. 16 and 17 for a $2B_{L_{o1}}$ = 100 Hz; and Figs. 18 and 19 for a $2B_{L_{o1}}$ = 300 Hz. The performance characteristics shown in these figures for the three-aperture array are similar to those discussed above for the two-aperture array for configurations representative of Figs. 1 and 2.

Initial measurements of enhanced RF carrier margin improvement have been made in the laboratory for two and three receiving systems arrayed. These measurements were made with a predetection filter noise bandwidth of 2200 Hz with a $2B_{L_{o1}}$ of 152 Hz for system 1 and with a $2B_{L_o}$ of 1 Hz with $k = 3.5$, $\gamma = 0.61$ for systems 2 and 3 (and $N_{o2}/N_{o1} = N_{o3}/N_{o1} = 1$). Measured enhanced RF carrier margin improvement was 1.3 dB with $\beta_2 = 0.56$ and $1 - \epsilon_1 = 0.73$ for two receiving systems arrayed (systems 1 and 2). This measurement was made with an initial RF carrier margin of 14.6 dB for receiving system 1 (prior to arraying). Predicted performance is 1.2 dB for $1 - \epsilon_1 = 0.73$ and 1.65 dB for $1 - \epsilon_1 = 1.0$ at this RF carrier margin for two systems arrayed. Measured enhanced RF carrier margin improvement was 2.2 dB with $\beta_2 = \beta_3 = 0.69$ and $1 - \epsilon_1 = 0.73$ for three receiving systems arrayed. This measurement was made with an initial RF carrier margin of 14 dB for receiving system 1 (prior to arraying). Predicted performance is 2.1 dB for $1 - \epsilon_1 = 0.73$ and 2.7 dB for $1 - \epsilon_1 = 1.0$ for three systems arrayed. Description of the laboratory measurement technique is presented in Ref. 1 (Section III).

The enhanced radio frequency carrier margin improvement for an array of receiving systems presented in this report results from a significant reduction in rms phase noise on the first local oscillator (the output of the RF carrier tracking loop) at a given input carrier level. This raises the point of switching operation to the next narrower bandwidth in the RF carrier tracking loop to accomplish essentially the same reduction in rms phase noise as with enhanced RF carrier margin improvement. Consider the following situation.

Receiving system 1 (with a 64-m diameter antenna) operating with a threshold two-sided noise bandwidth ($2B_{L_{o1}}$) of 30 Hz has an initial carrier margin (carrier level above design-point threshold) of 10 dB by itself prior to arraying. When arrayed with a second receiving system (with a 34-m diameter antenna) with $k = 9$, the improvement in 64-m receiver carrier margin is 4.8 dB for an array configuration representative of Fig. 1 (see Fig. 7). The resultant receiver array enhanced carrier margin is 10 + 4.8 or 14.8 dB. Receiving system 1 operating with a $2B_{L_o}$ of 10 Hz would have a carrier margin of 14.77 dB since the ratio of 30/10 represents 4.77 dB. Comparison of the doppler rate capability for a given phase error (e.g., 10 deg) due to doppler rate shows that the enhanced carrier margin array ($2B_{L_{o1}}$ = 30 Hz) has 2.9 times the doppler rate capability of receiving system 1 with $2B_{L_{o1}}$ = 10 Hz. This ratio increases to 5.4 at strong signals. A similar comparison for $k = 9$ and $2B_{L_{o1}}$ equal to 100 Hz (see Fig. 9) for the enhanced carrier margin array as compared to receiving system 1 operating with a $2B_{L_{o1}}$ of 30 Hz provides a 3.9 times doppler rate capability. In this case, the ratio increases to 18.6 at strong signals. This last doppler rate comparison also applies for $2B_{L_{o1}}$ equal to 10 Hz for the enhanced carrier margin array ($K = 9$) as compared to receiving system 1 operating with a $2B_{L_{o1}}$ of 3 Hz.

V. Discussion

Enhanced RF carrier margin improvement for arrayed receiving systems is shown for values of k up to 70 in Section IV of this report. It should be noted that application of the parameters described herein to receiving equipment presently at the 64-m stations requires some limits on the maximum value of k. A value of k up to 70 can be accommodated for threshold two-sided noise bandwidths ($2B_{L_{o1}}$) of 10 and 30 Hz. However, for $2B_{L_{o1}}$ equal to 100 and 300 Hz, the maximum value of k is limited to 8 or 9.

The additional RF carrier sensitivity realized by enhanced carrier margin improvement provides a performance capability (illustrated below) that should be investigated and verified by further laboratory measurements. As an illustration, the performance in Fig. 4 shows the improvement in the 64-m receiving system carrier margin for an array of two receiving system utilizing a 64-m diameter antenna and a 34-m diameter antenna-listen only. For $k = 9$, this array should acquire the RF carrier when the initial 64-m receiver carrier margin is as low as 5.5 dB. After RF carrier acquisition at this (5.5 dB) level, the effective RF carrier margin of the 64-m receiver (arrayed) would be 10.8 dB (5.5 + 5.3 dB) as determined by rms phase (σ_{ϕ_n}) in the RF carrier phase tracking loop.

The following situation is presented to illustrate an application of enhanced RF carrier margin improvement during the fly-by encounter of a spacecraft with a planet in the solar system. When operating with a modulation index of 72 deg peak, the RF carrier margin for the 64-m diameter antenna receiving system at an elevation angle of 31 deg is 17.7 dB when operation with a $2B_{L_{o1}}$ = 30 Hz (clear dry weather). This is representative for the 64-m antenna at the Goldstone complex with Voyager 2 at Neptune.[1] Increasing the peak

[1] Voyager Telecom Data Base, Design Control Table, $P_T = -138.1$ dBm at Uranus, T_{op} = 26.7 K at DSS-14, 31 deg elevation angle, clear dry weather. Signal level is 3.5 dB less at Neptune (private communication with B. D. Madsen, JPL).

modulation index to 80 deg decreases the RF carrier margin by 5 dB and increases the received telemetry signal-to-noise ratio by 0.30 dB. The RF carrier margin is reduced 2 dB at an antenna elevation angle of approximately 17 deg relative to a 31 deg elevation angle.

Table 1 shows the RF carrier margin for the 64-m diameter antenna receiving system by itself ($2B_{L_{o1}}$ = 30 Hz) at antenna elevation angles of approximately 31 and 17 deg for peak modulation indices of 72 and 80 deg. Radio loss is also shown in Table 1 for the above antenna elevation angles and modulation indices for short constraint length (7), rate 1/2 convolutional coded telemetry (Ref. 3, Figs. 14 and 3) for an array consisting of a 64-m diameter antenna and a 34-m diameter-listen only antenna. Radio loss is shown for baseband arraying and for an array with both enhanced RF carrier margin improvement and baseband arraying. Enhanced RF carrier margin improvement is obtained from Fig. 7 (Fig. 1 configuration). Because of the 64-m enhanced carrier margin, the radio loss is less for this case.

The preceeding discussion has assumed that the doppler rate (due to range acceleration), as seen at the DSN complex, produces a small phase error in the RF carrier phase tracking loops of the 64-m and 34-m receiving systems. This is true (small phase error) except during the time period when range acceleration peaks. For a few hours during fly-by of the planet (Neptune), the two-way X-band doppler rate increases to a peak of about 170 Hz/s and then decreases to less than 0.1 this value (A. B. Sergeysky, D. M. Wegener, and R. J. Cesarone, private communication). Consider the baseband array with a 17.7 dB carrier margin for the 64-m antenna receiving system and 17.7 - 4.3 = 13.4 dB carrier margin for the 34-m antenna-listen only receiving system ($2B_{L_{o1}}$ = 30 Hz, 72 deg modulation index and antenna elevation angle approximately 31 deg). The resultant phase errors due to a doppler rate of 170 Hz/s are 13 and 19 deg in the RF carrier phase tracking loop for the 64-m and 34-m antenna receiving systems, respectively. At an antenna elevation angle of approximately 17 deg, the RF carrier tracking loop phase errors become 16 and 23 deg, respectively. Consider next, the array with both enhanced RF carrier margin improvement and base-band arraying operating with a $2B_{L_{o1}}$ = 100 Hz and k = 9. At an antenna elevation angle of approximately 31 deg, the phase error in the RF carrier phase tracking loop is 3 deg (due to 170 Hz/s) and the enhanced RF carrier margin of the 64-m antenna receiver is 17.6 dB (12.5 + 5.1 dB) from Fig. 9 (Fig. 1 configuration). At an antenna elevation angle of approximately 17 deg the phase error is 4 deg and the enhanced RF carrier margin of the 64-m antenna receiver is 17.2 dB (10.5 + 6.7 dB).

References

1. Brockman, M. H., The Effect of Partial Coherence in Receiving System Noise Temperature on Array Gain for Telemetry and Radio Frequency Carrier Reception for Receiving Systems with Unequal Predetection Signal-to-Noise Ratios, *TDA Progress Report 42-72*, pp. 95-117, Jet Propulsion Laboratory, Pasadena, California, February 15, 1983.

2. Brockman, M. H., The Effect of Partial Coherence in Receiving System Noise Temperature on Array Gain for Telemetry and Radio Frequency Carrier Reception for Similar Receiving Systems, *TDA Progress Report 42-66*, pp. 219-235, Jet Propulsion Laboratory, Pasadena, California, December 15, 1981.

3. Divsalar, D., and Yuen, J. H., Improved Carrier Tracking Performance with Coupled Phase-Locked Loops, *TDA Progress Report 42-66*, pp. 148-171, Jet Propulsion Laboratory, Pasadena, California, December 15, 1981.

Table 1. 64-m and 34-m (listen only) antenna receiver array ($2B_{L_o}$ = 30 Hz)

Antenna Elev. Angle, deg	Modulation Index, deg. peak	Single 64-m Carrier Margin, dB	Baseband Array Radio Loss, dB		Enhanced Carrier Margin and Baseband Array			
			BER 5×10^{-3}	BER 5×10^{-5}	k	64-m Enhanced Carrier Margin, dB	Radio Loss, dB	
							BER 5×10^{-3}	BER 5×10^{-5}
~31	72	17.7	~0.25	~0.5	9	21.	~0.05	~0.1
					18	22.	~0.05	~0.1
	80	12.7	~1.3	~3.5	9	17.1	~0.25	~0.4
					18	18.4	~0.2	~0.25
~17	72	15.7	~0.45	~0.9	9	19.5	~0.1	~0.15
					18	20.6	<0.1	~0.1
	80	10.7	*	*	9	15.4	~0.4	~1.0
					18	16.8	~0.3	~0.4

*34-m receiver cycle slipping

Convolutional coded telemetry
Short constraint length (7)
Rate 1/2
$Q = 3$

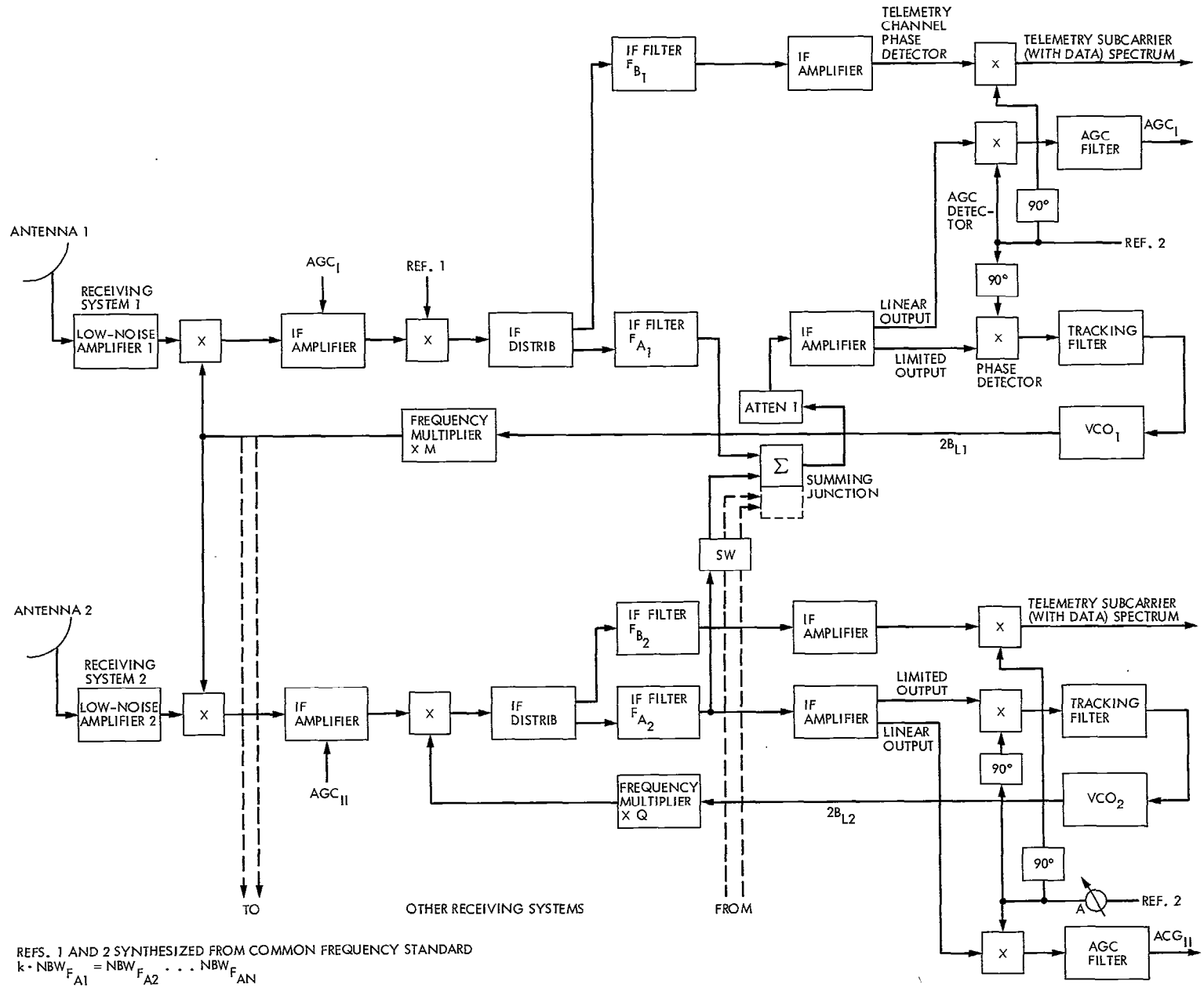

Fig. 1. Enhanced radio frequency carrier arraying

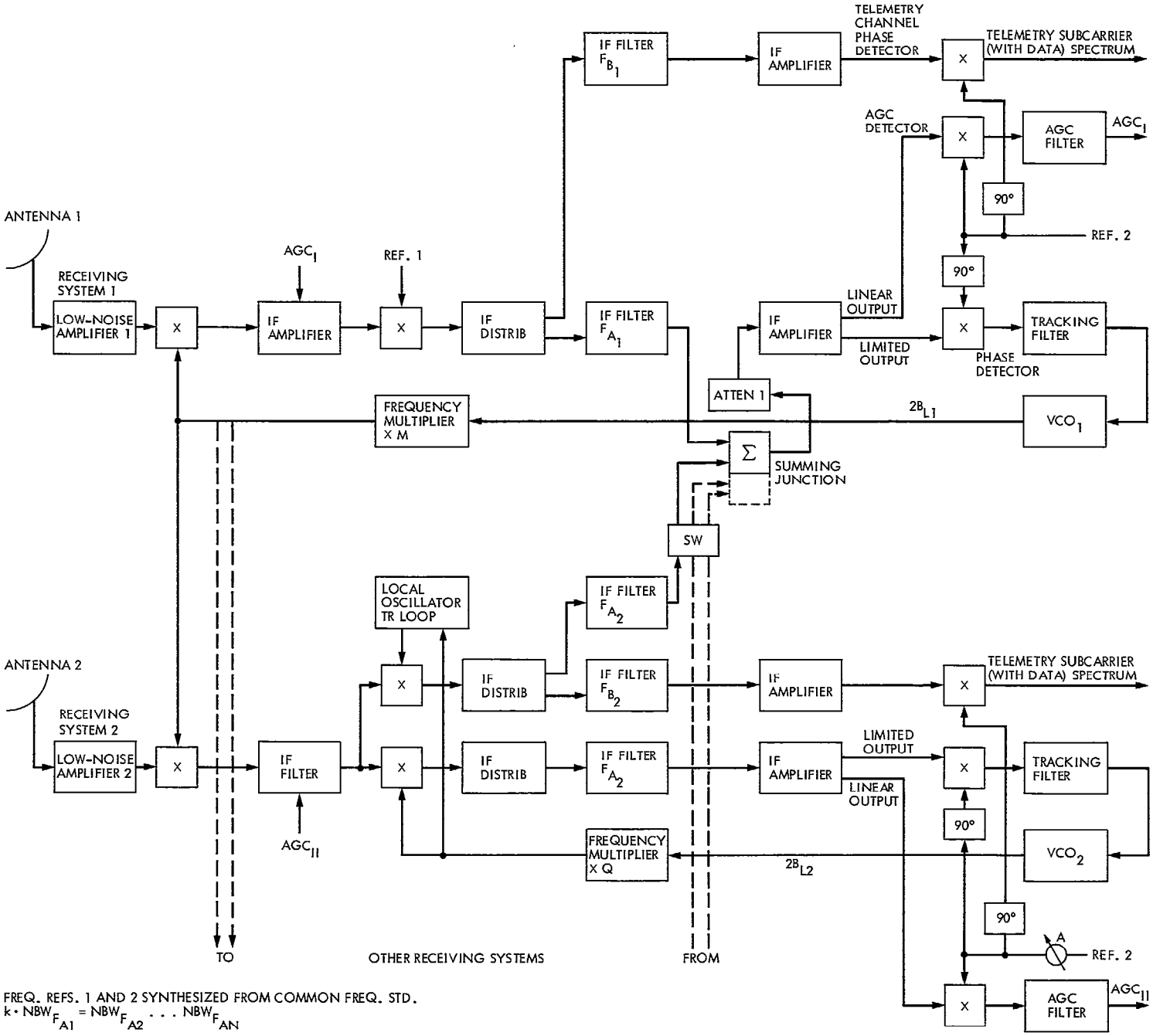

FREQ. REFS. 1 AND 2 SYNTHESIZED FROM COMMON FREQ. STD.
$k \cdot NBW_{F_{A1}} = NBW_{F_{A2}} \ldots NBW_{F_{AN}}$

Fig. 2. Enhanced radio frequency carrier arraying with additional local oscillator filtering

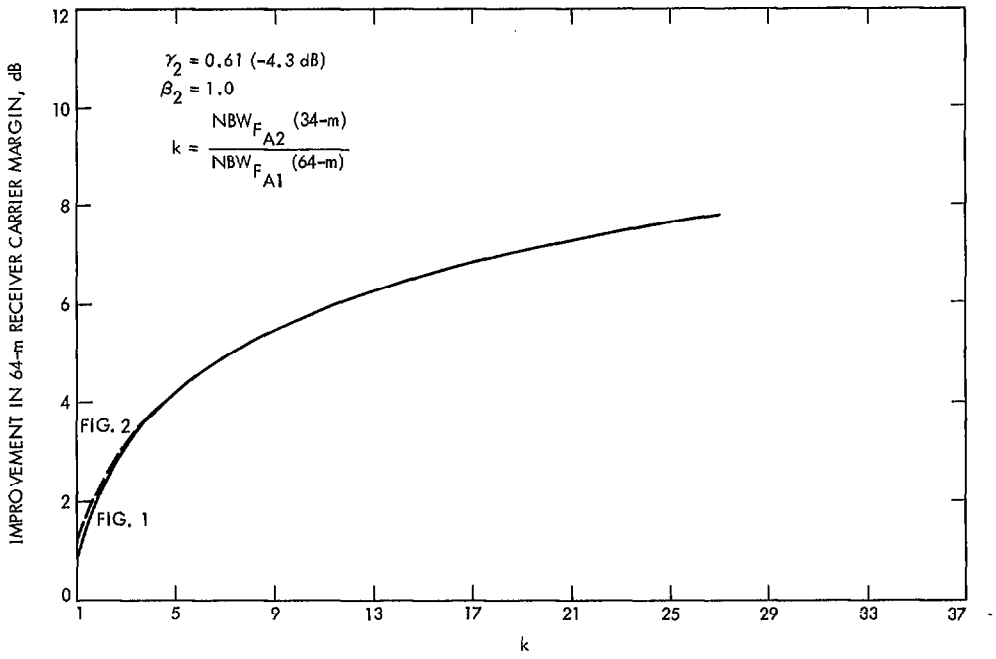

Fig. 3. Enhanced RF carrier margin improvement vs k ($2B_{L/o1}$ = 10. Hz). Two receiving systems are arrayed, the 64-m and 34-m (listen-only) diameter antennas. The 64-m was initially at 10-dB carrier margin.

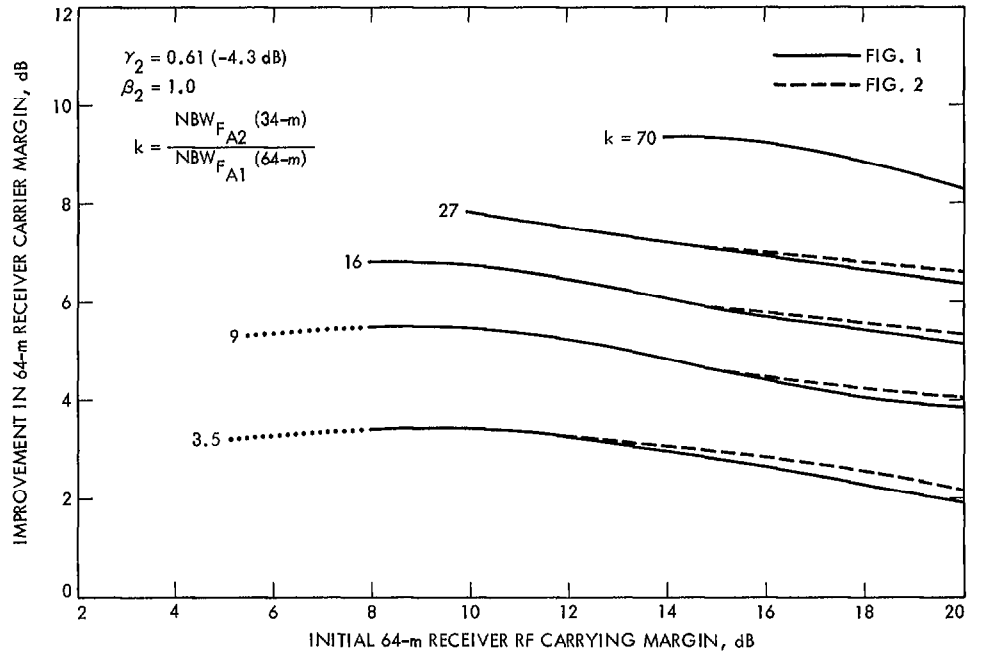

Fig. 4. Enhanced RF carrier margin improvement vs initial 64-m receiver carrier margin ($2B_{L/o1}$ = 10. Hz). Two receiving systems are arrayed, the 64-m and 34-m (listen-only) diameter antennas.

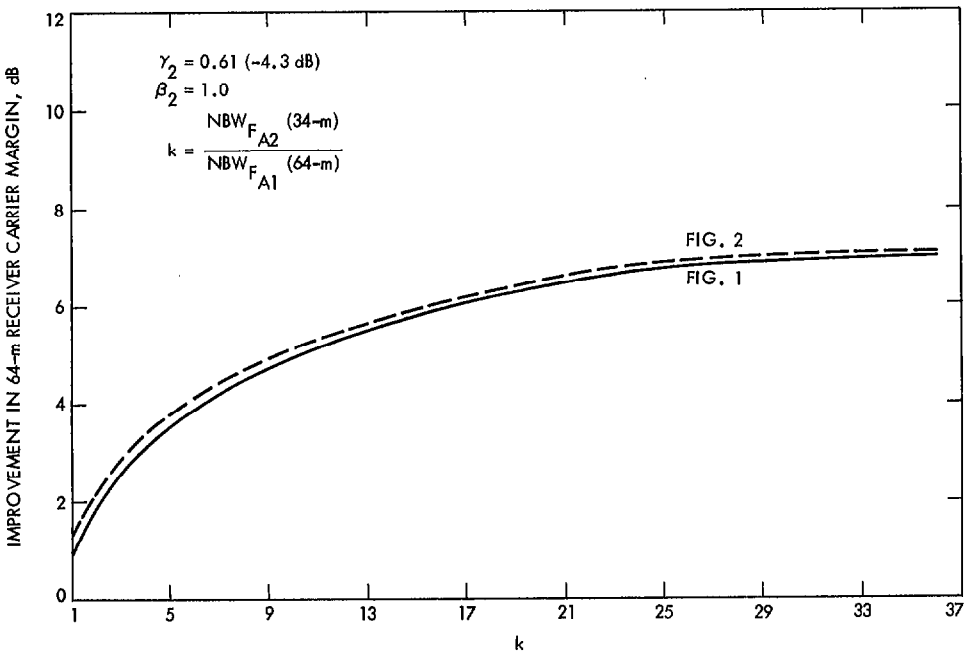

Fig. 5. Enhanced RF carrier margin improvement vs k ($2B_{L/o1}$ = 30. Hz). Two receiving systems are arrayed, the 64-m and 34-m (listen-only) diameter antennas. The 64-m was initially at 10-dB carrier margin.

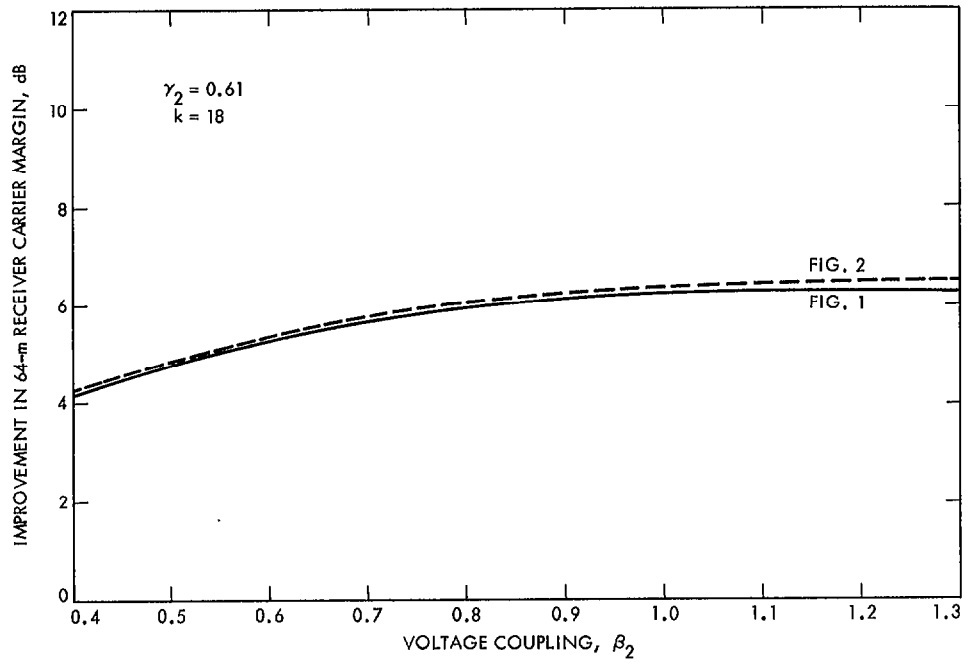

Fig. 6. Effect of summing junction voltage coupling on enhanced RF carrier margin improvement. Two receiving systems are arrayed, the 64-m and 34-m (listen-only) diameter antennas. The 64-m was initially at 10-dB carrier margin ($2B_{L/o1}$ = 30. Hz).

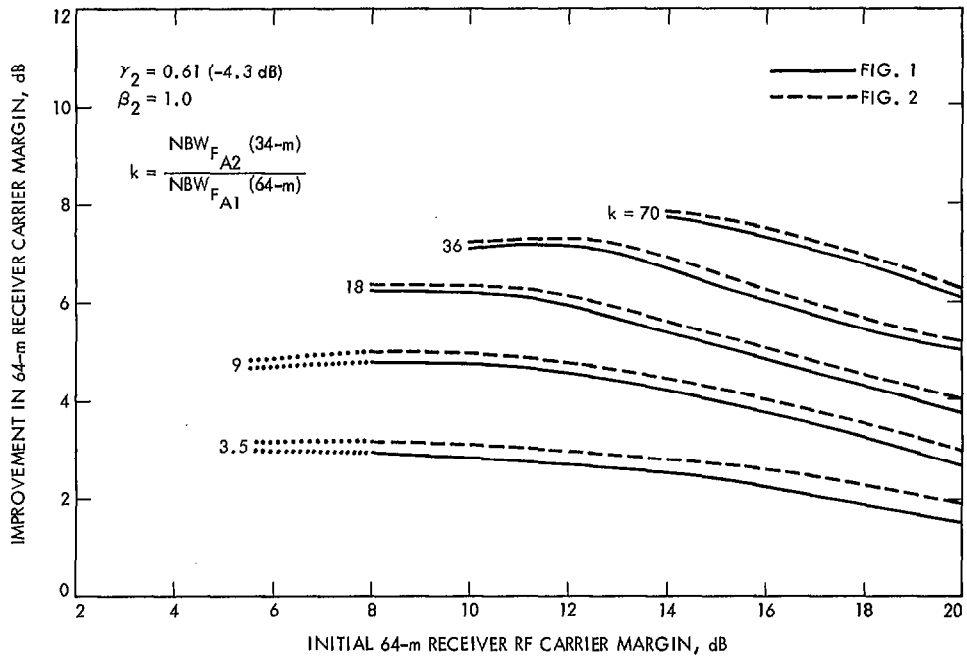

Fig. 7. Enhanced RF carrier margin improvement vs initial 64-m receiver RF carrier margin ($2B_{L/o1}$ = 30. Hz). Two receiving systems are arrayed, the 64-m and 34-m (listen-only) diameter antennas.

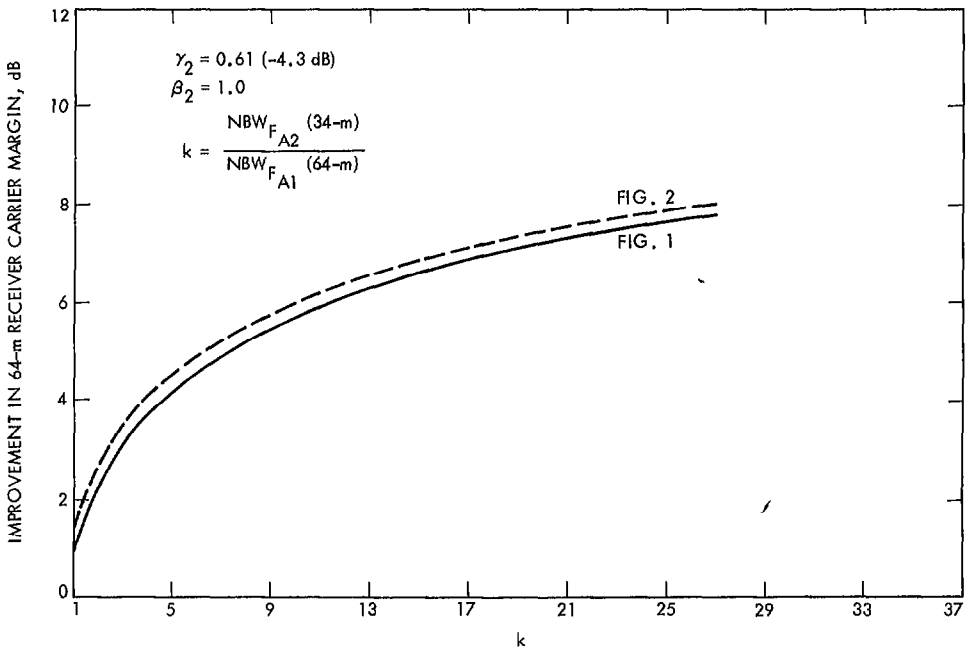

Fig. 8. Enhanced RF carrier margin improvement vs *k* ($2B_{L/o1}$ = 100. Hz). Two receiving systems are arrayed, the 64-m and 34-m (listen-only) diameter antennas. The 64-m was initially at 10-dB carrier margin.

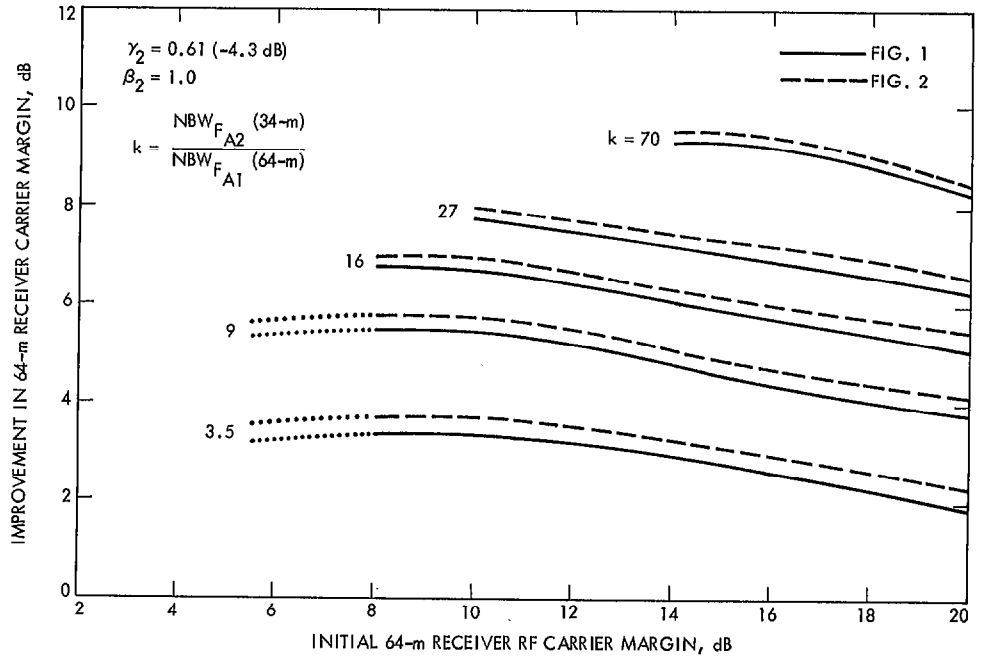

Fig. 9. Enhanced RF carrier margin improvement vs initial 64-m receiver RF carrier margin ($2B_{L/o1}$ = 100. Hz). Two receiving systems are arrayed, the 64-m and 34-m (listen-only) diameter antennas.

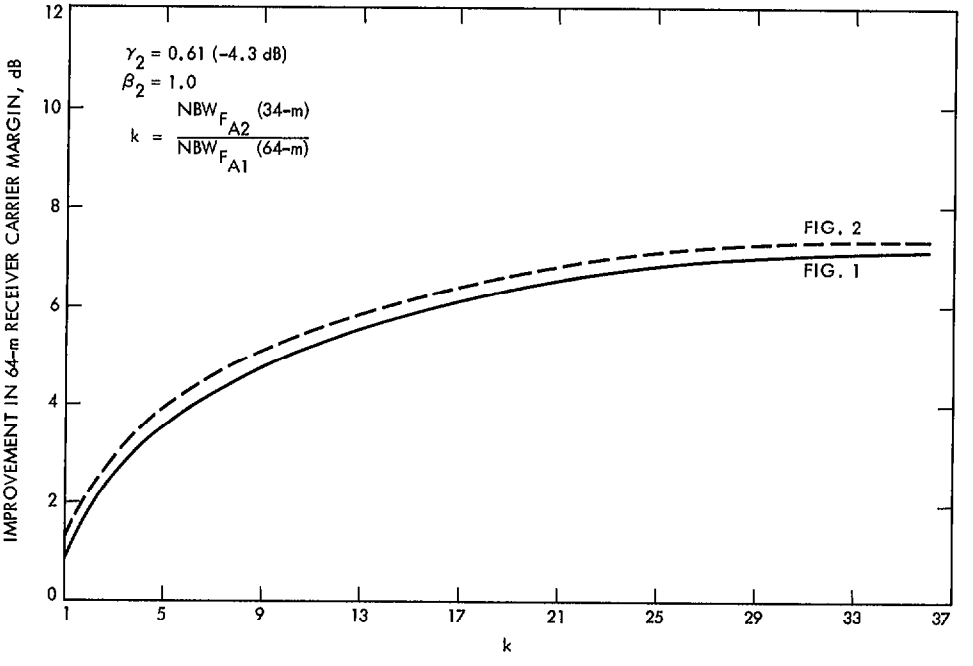

Fig. 10. Enhanced RF carrier margin improvement vs *k* ($2B_{L/o1}$ = 300. Hz). Two receiving systems are arrayed, the 64-m and 34-m (listen-only) diameter antennas. The 64-m was initially at 10-dB carrier margin.

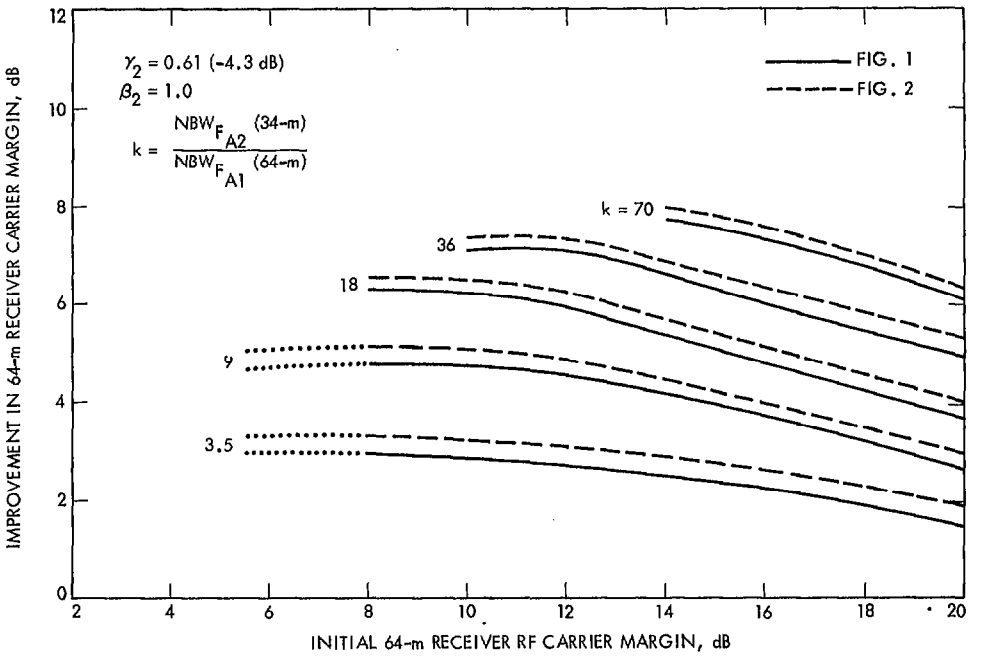

Fig. 11. Enhanced RF carrier margin improvement vs initial 64-m receiver RF carrier margin ($2B_{L/o1}$ = 300. Hz). Two receiving systems are arrayed, the 64-m and 34-m (listen-only) diameter antennas.

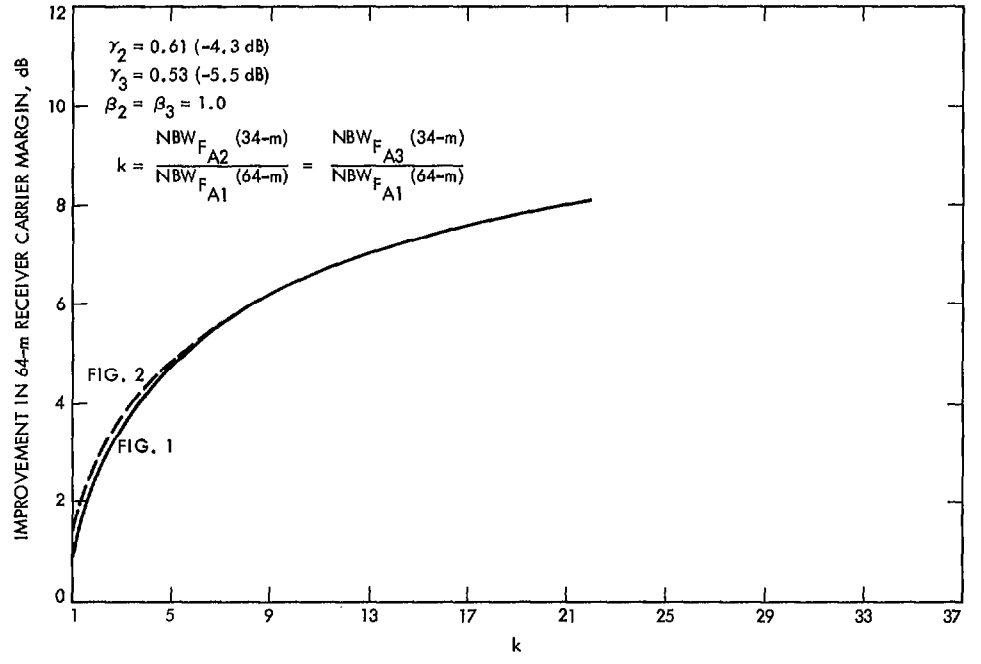

Fig. 12. Enhanced RF carrier margin improvement vs k ($2B_{L/o1}$ = 10. Hz). Three receiving systems are arrayed, the 64-m, 34-m (listen-only), and 34-m (transmit/receive) diameter antennas. The 64-m was initially at 10-dB carrier margin.

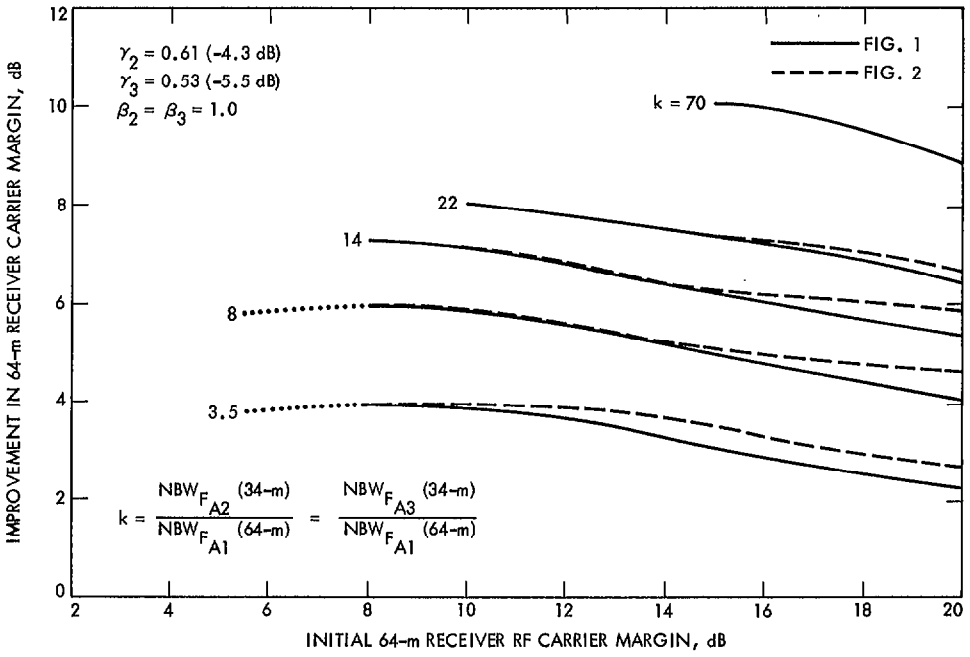

Fig. 13. Enhanced RF carrier margin improvement vs initial 64-m receiver RF carrier margin ($2B_{L/o1}$ = 10. Hz). Three receiving systems are arrayed, the 64-m, 34-m (listen-only), and 34-m (transmit/receive) diameter antennas.

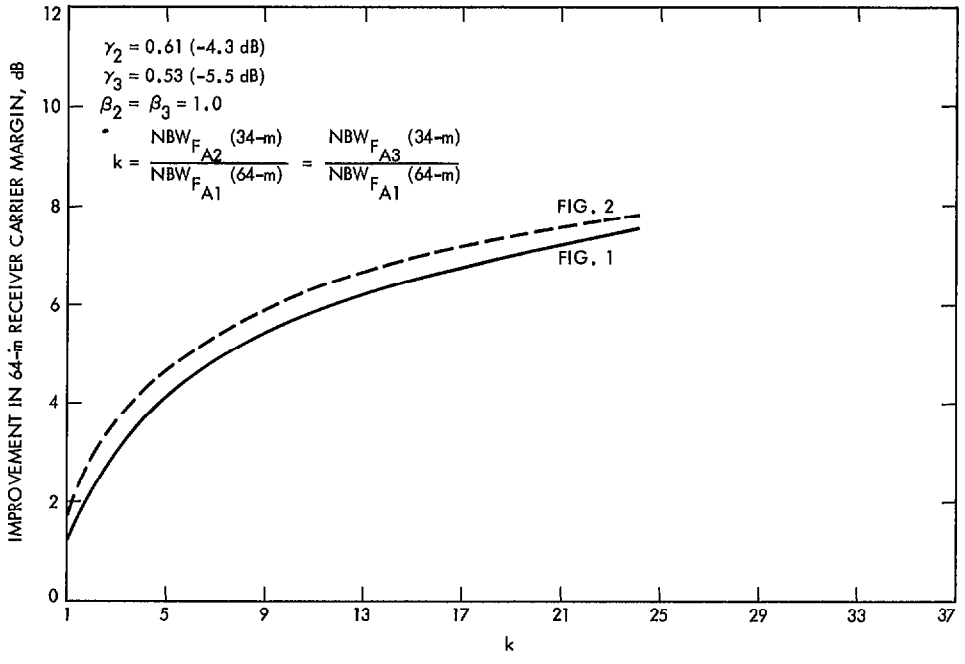

Fig. 14. Enhanced RF carrier margin improvement vs *k* ($2B_{L/o1}$ = 30. Hz). Three receiving systems are arrayed, the 64-m, 34-m (listen-only), and 34-m (transmit/receive) diameter antennas. The 64-m was initially at 10-dB carrier margin.

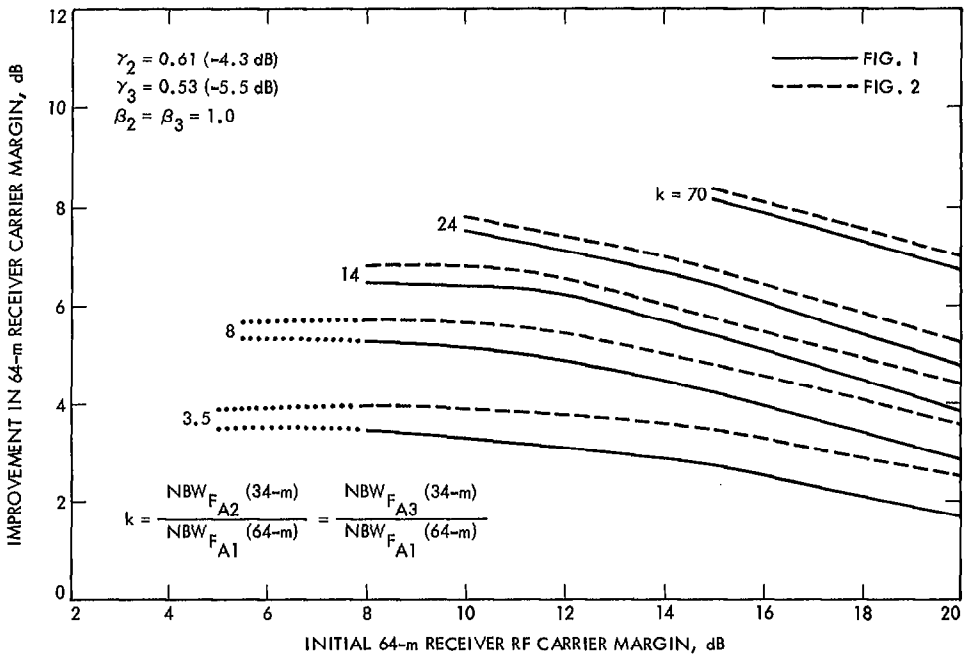

Fig. 15. Enhanced RF carrier margin improvement vs initial 64-m receiver RF carrier margin ($2B_{L/o1}$ = 30. Hz). Three receiving systems are arrayed, the 64-m, 34-m (listen-only), and 34-m (transmit/receive) diameter antennas.

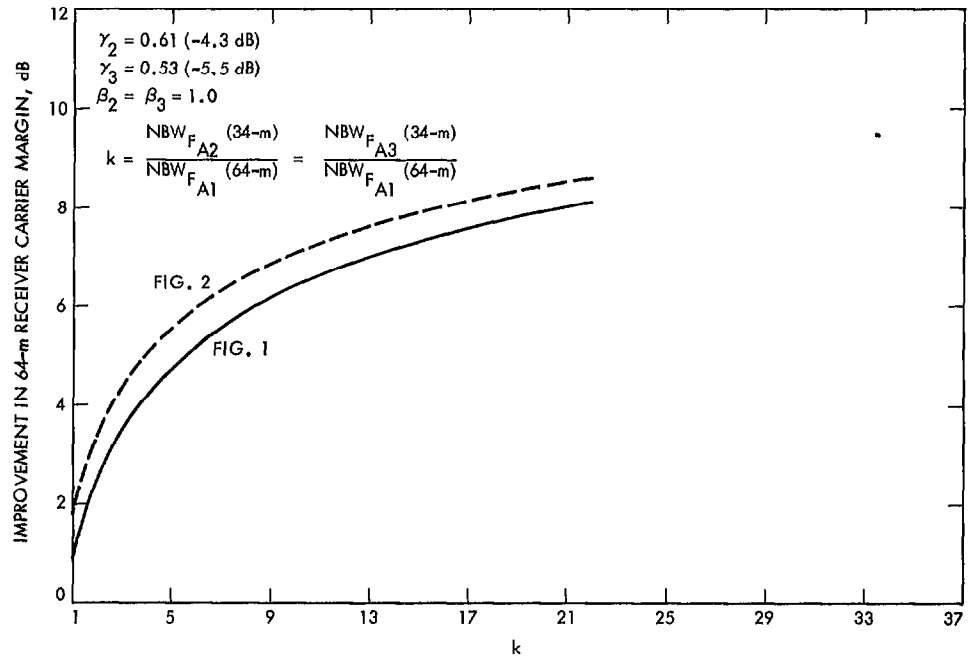

Fig. 16. Enhanced RF carrier margin improvement vs *k* ($2B_{L/o1}$ = 100. Hz). Three receiving systems are arrayed, the 64-m, 34-m (listen-only), and 34-m (transmit/receive) diameter antennas. The 64-m was initially at 10-dB carrier margin.

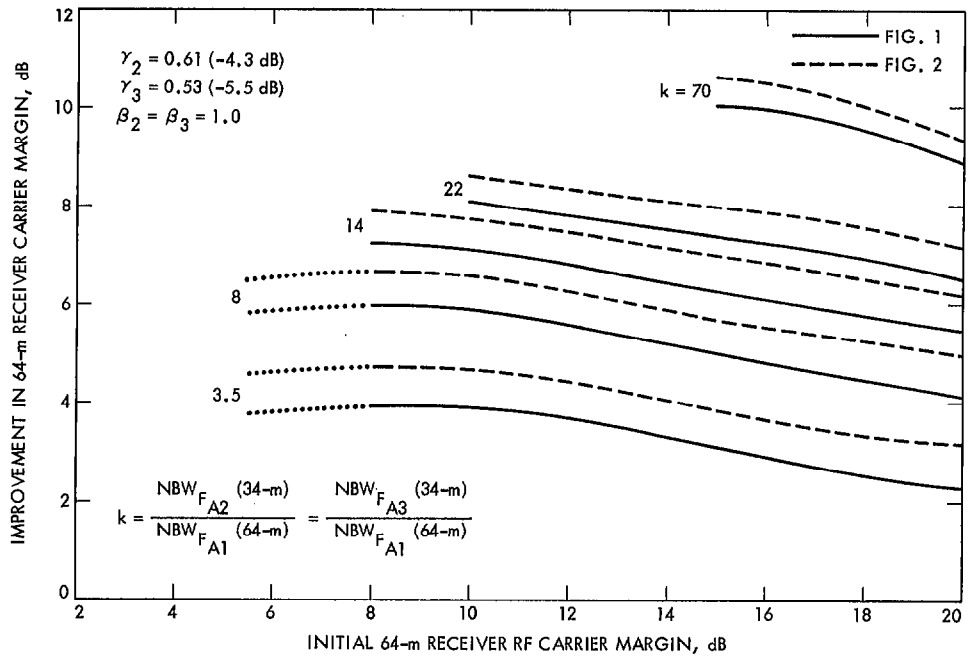

Fig. 17. Enhanced RF carrier margin improvement vs initial 64-m receiver RF carrier margin ($2B_{L/o1}$ = 100. Hz). Three receiving systems are arrayed, the 64-m, 34-m (listen-only), and 34-m (transmit/receive) diameter antennas.

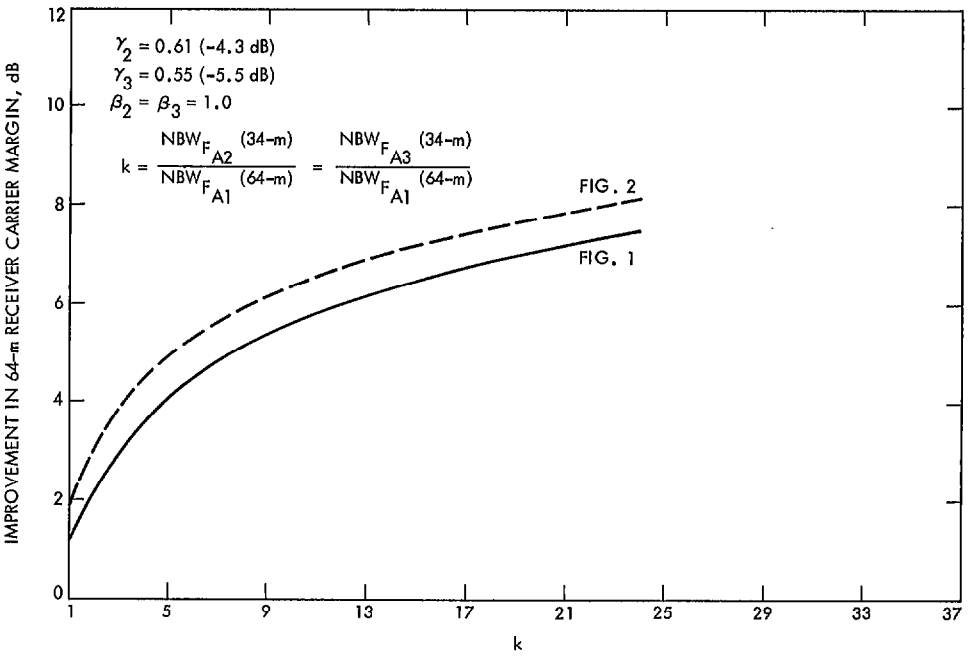

Fig. 18. Enhanced RF carrier margin improvement vs k ($2B_{L/o1}$ = 300. Hz). Three receiving systems are arrayed, the 64-m, 34-m (listen-only), and 34-m (transmit/receive) diameter antennas. The 64-m was initially at 10-dB carrier margin.

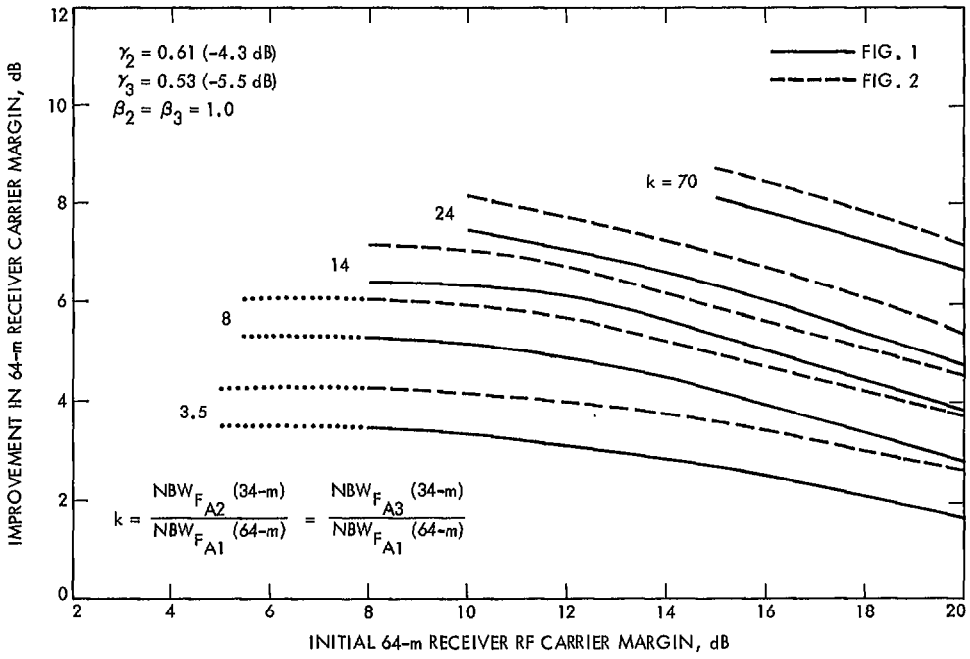

Fig. 19. Enhanced RF carrier margin improvement vs initial 64-m receiver RF carrier margin ($2B_{L/o1}$ = 300. Hz). Three receiving systems are arrayed, the 64-m, 34-m (listen-only), and 34-m (transmit/receive) diameter antennas.